FIRS FOV

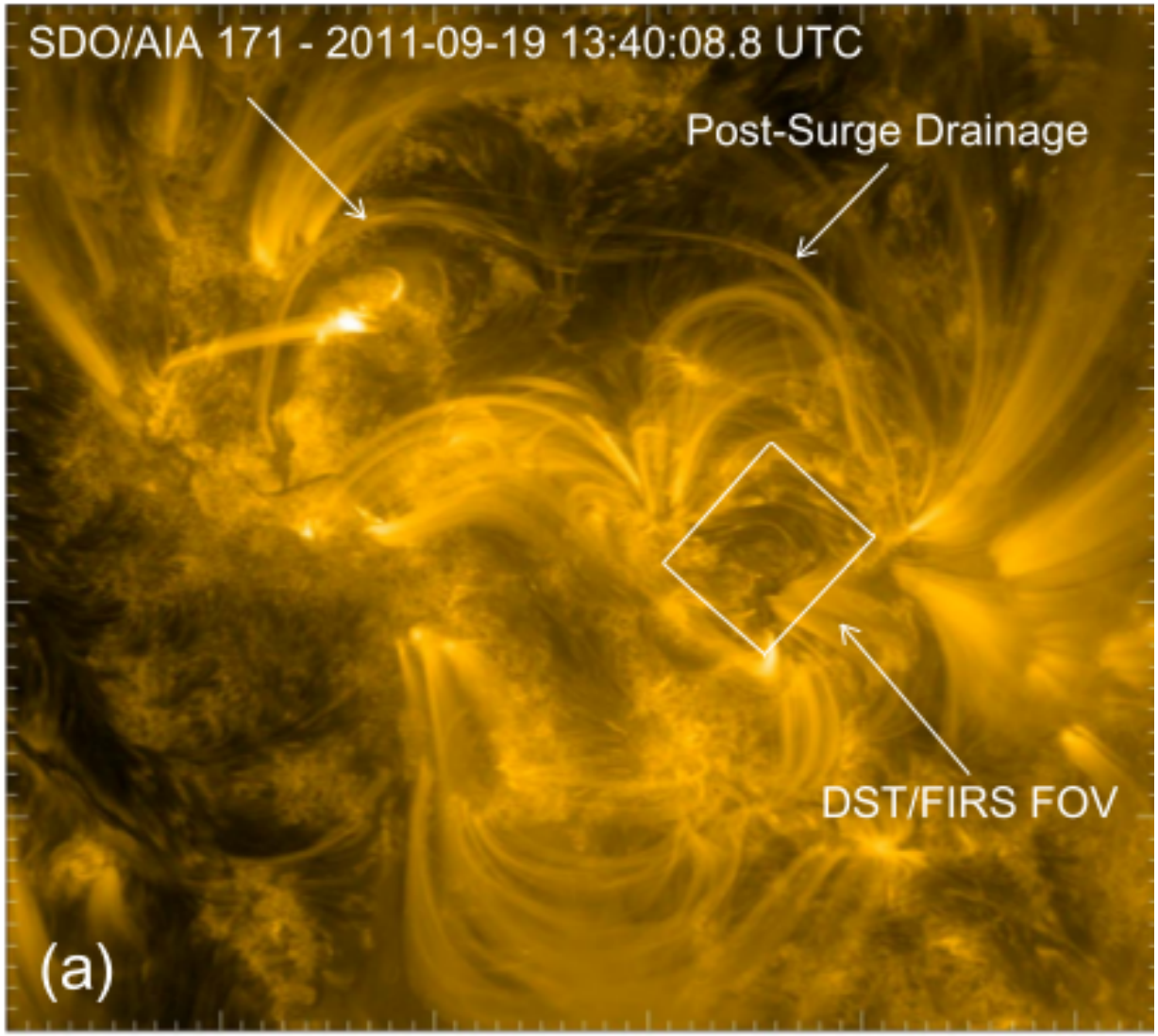
SDO/AIA 171 - 2011-09-19 13:40:08.8 UTC
Post-Surge Drainage
DST/FIRS FOV
(a)

FIRS FOV

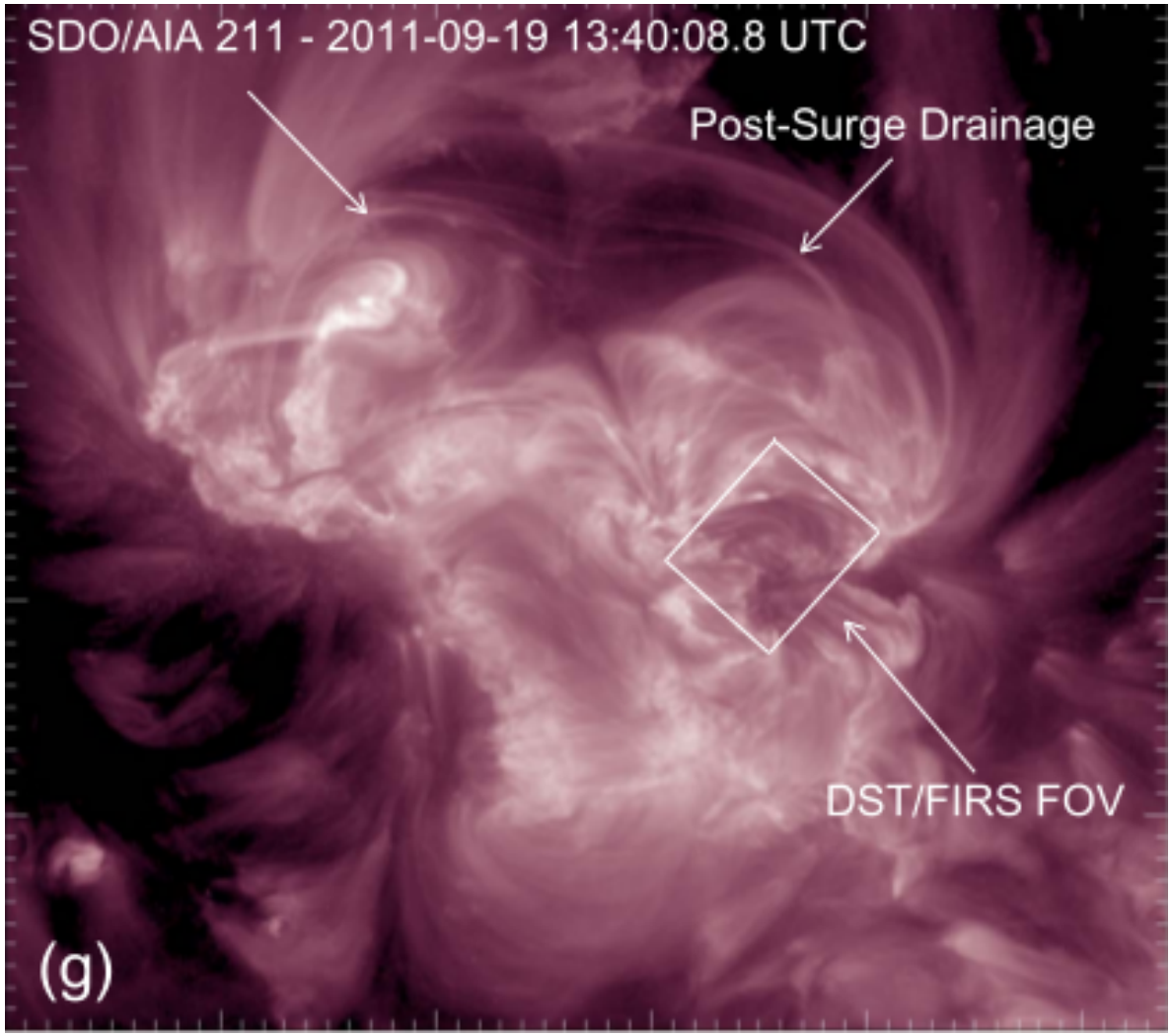
SDO/AIA 211 - 2011-09-19 13:40:08.8 UTC
Post-Surge Drainage
DST/FIRS FOV
(g)

FIRS data

- field of view of 60x70 arcsec
- the slit was oriented at a 41.3 deg. angle with respect to the solar meridian
- spatial sampling of 0.29 arcsec and an observed spectral range of 35.743 $\mathring{A}(\Delta\lambda = 8.683 m\mathring{A}/pixel)$
- the slit was scanned from solar northeast to southwest with a step size equal to the projected slit width of 0.29 arcsec
- At each slit position, spectra were acquired using a sequence of four efficiency-balanced modulation states using 125 ms exposures, which was repeated once for a total of 1 s cumulative integration time. The 218 step scan lasted 32 minutes

FIRS data

time of slit scan: 16:29 - 17:01

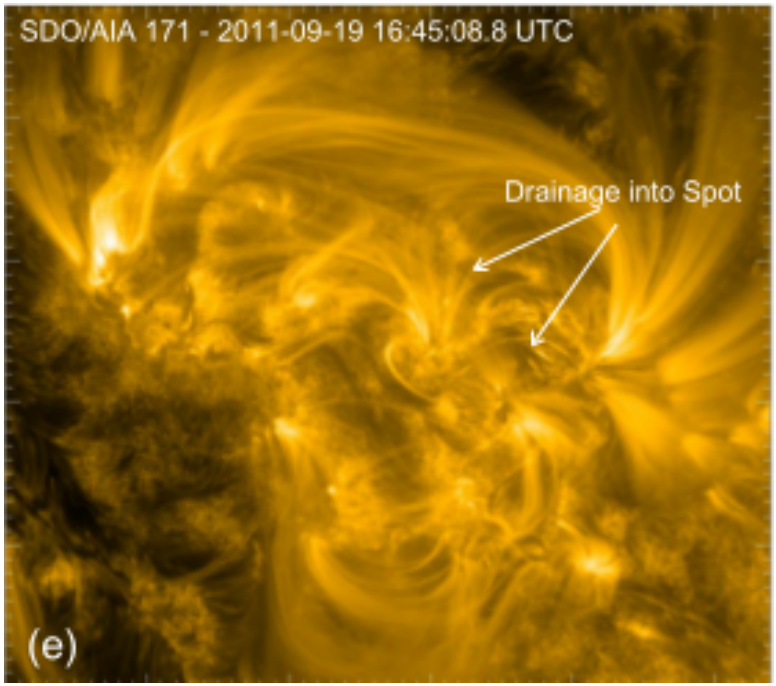

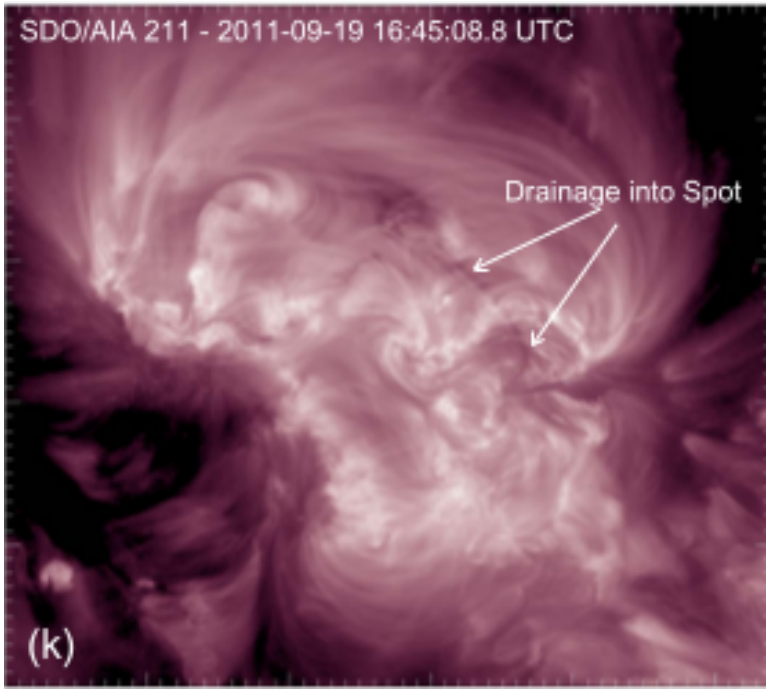

FIRS data

Standard reduction methods were applied to the FIRS data in the manner described by Schad et al. (2013), which includes dark and flat calibrations, geometric registration, wavelength calibration, and polarimetric cross-talk removal. One exception here is that the spectral dispersion was determined by fitting the line cores of the two telluric lines at 10833.981 and 10832.108 Å, as in Kuckein et al. (2012b). Residual interference fringes were removed from the polarized spectra using the 2D pattern recognition technique of Casini et al. (2012), resulting in an unbinned mean noise level in Stokes (Q, U, V) of (1.0, 0.92, 1.3)10^{-3} , in units of the incident intensity. The reference direction for Stokes+Q is parallel to the solar equator.

FIRS data

Despite real-time seeing correction and image stabilization by the DST high-order adaptive optics system (Rimmele et al. 2004), the solar image experienced shifts up to 0.1 arcsec between adjacent FIRS slit positions due to short periods of degraded atmospheric seeing, with a cumulative temporal drift of 2.55 arcsec during the scan. These shifts have been corrected through careful image registration with a co-operating G-band context imager. Image shifts determined from the G-band images are converted to their equivalent shift within the FIRS map.

Any spatial maps of feature topology or physical quantities derived from the FIRS maps are corrected using Delaunay triangulation of the translated observation points (Lee, Schachter 1980) and subsequent quintic-polynomial smooth interpolation

He velocity along loop

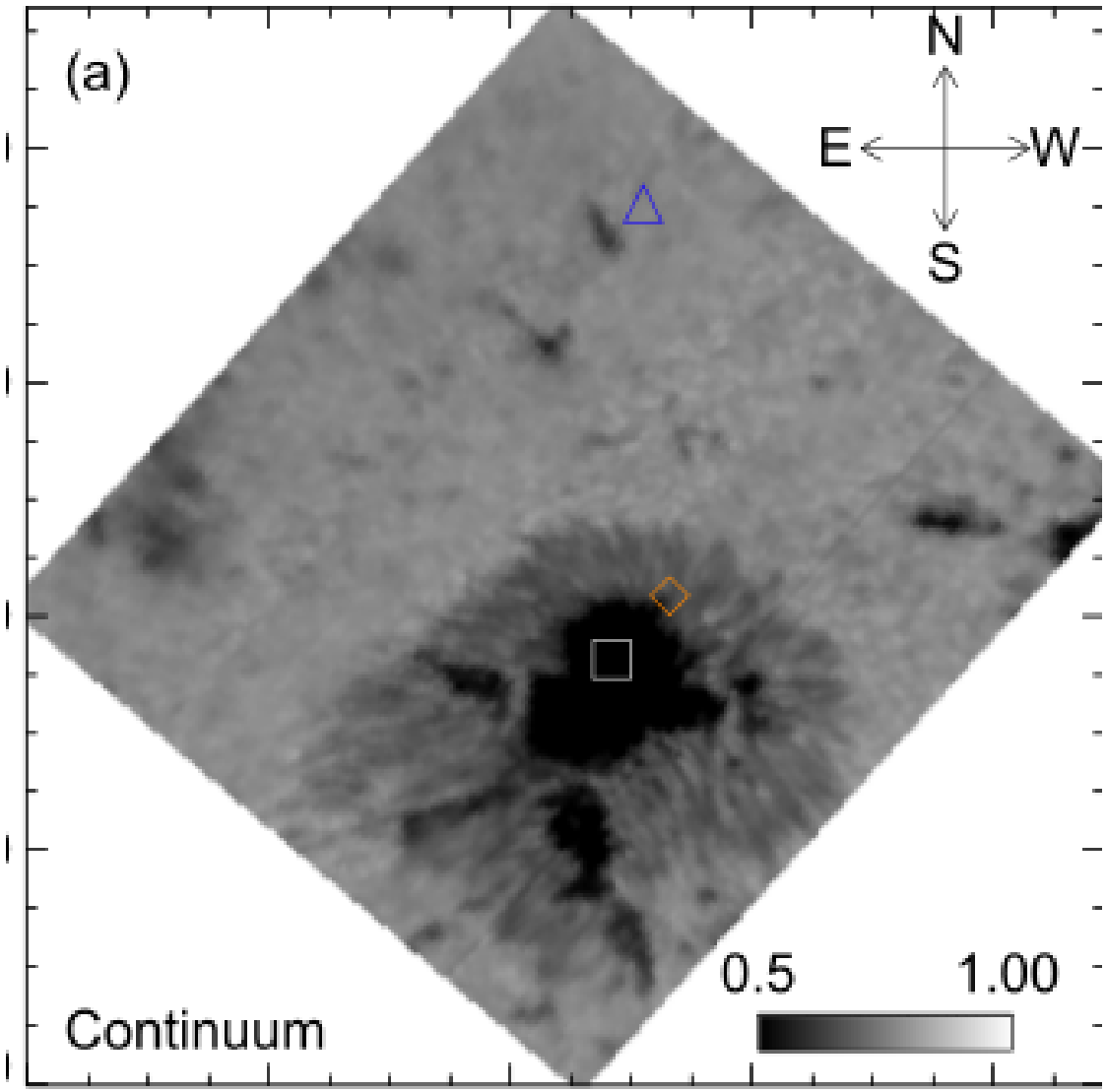

He velocity along loop

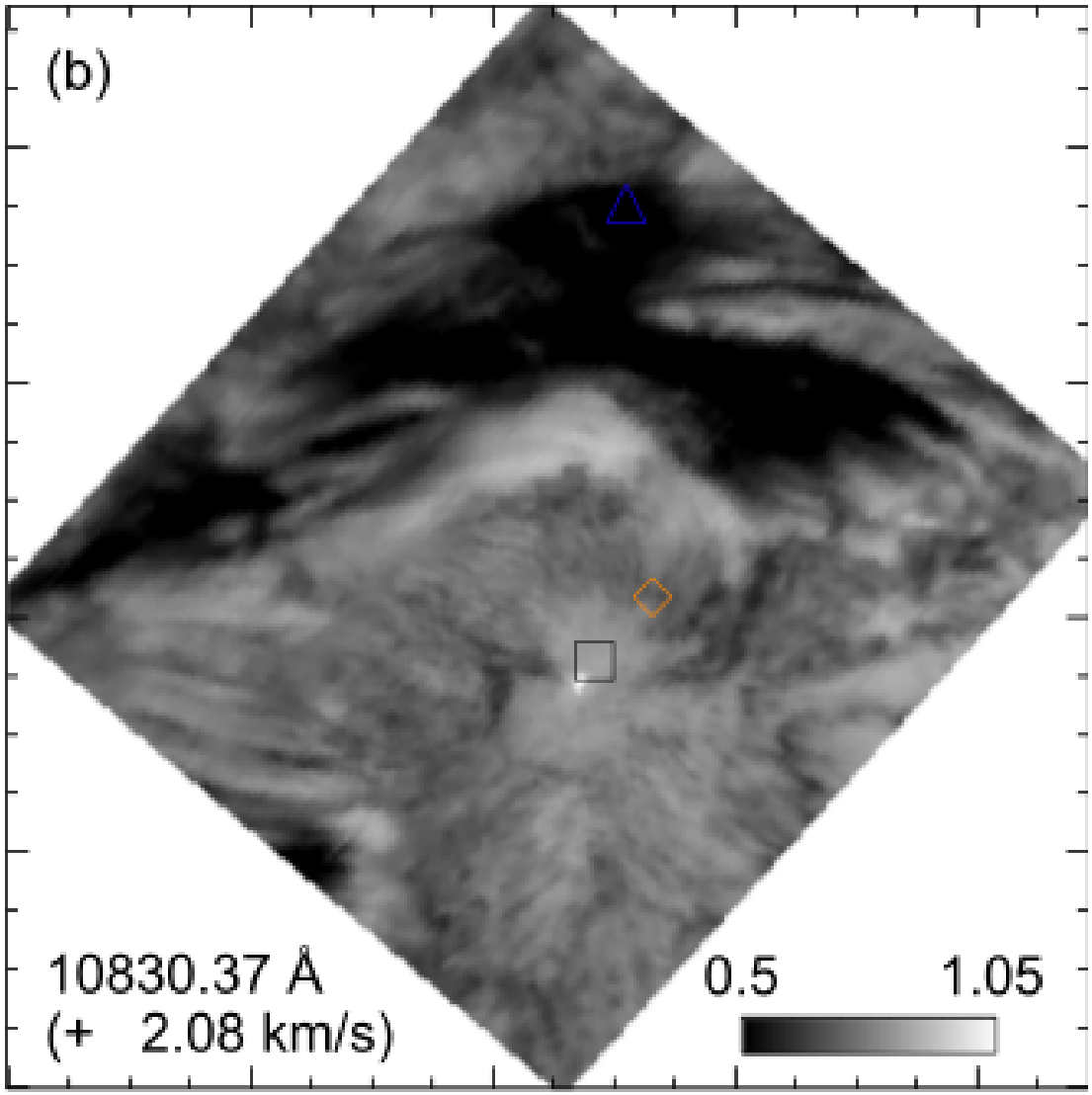

He velocity along loop

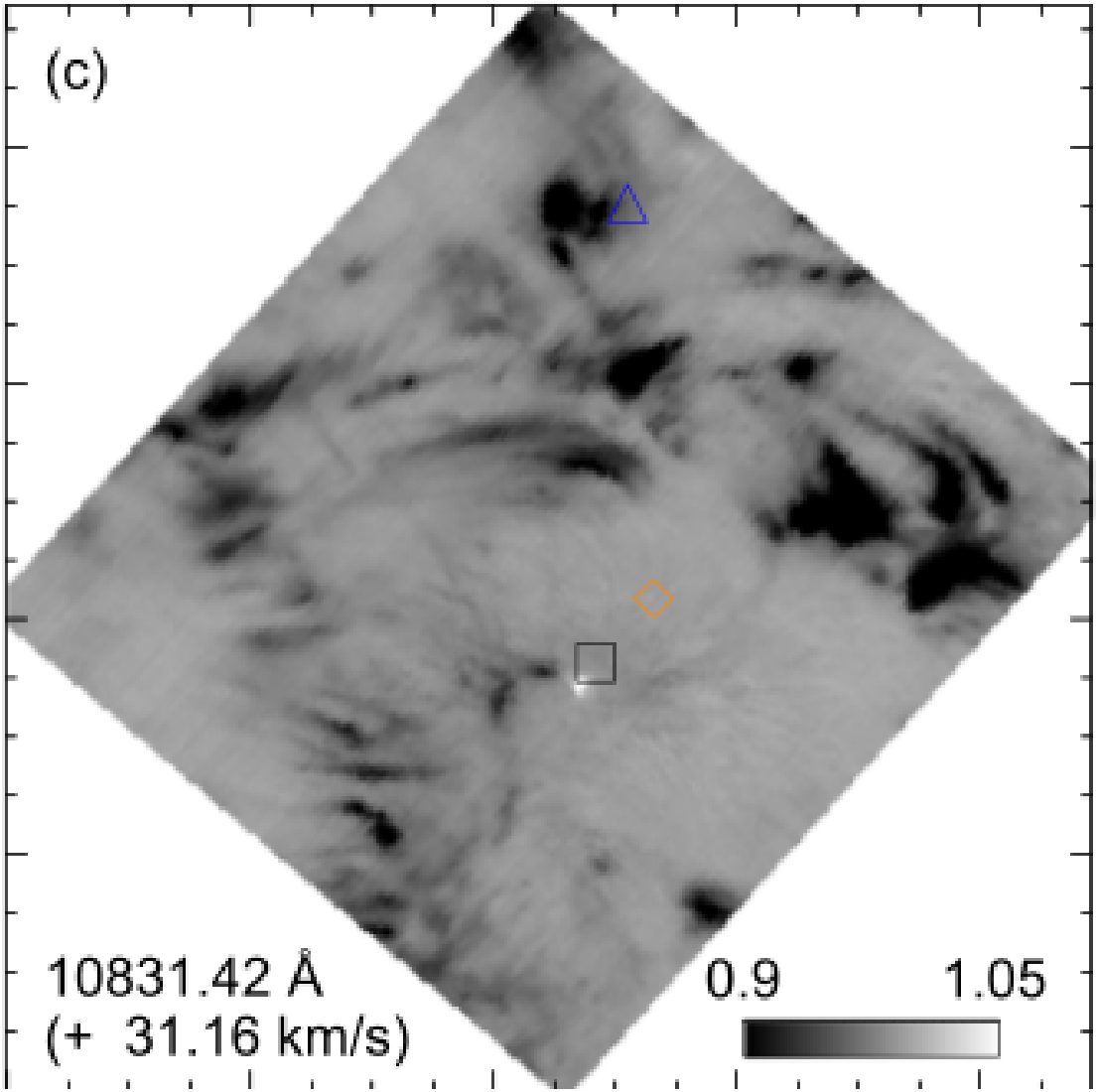

He velocity along loop

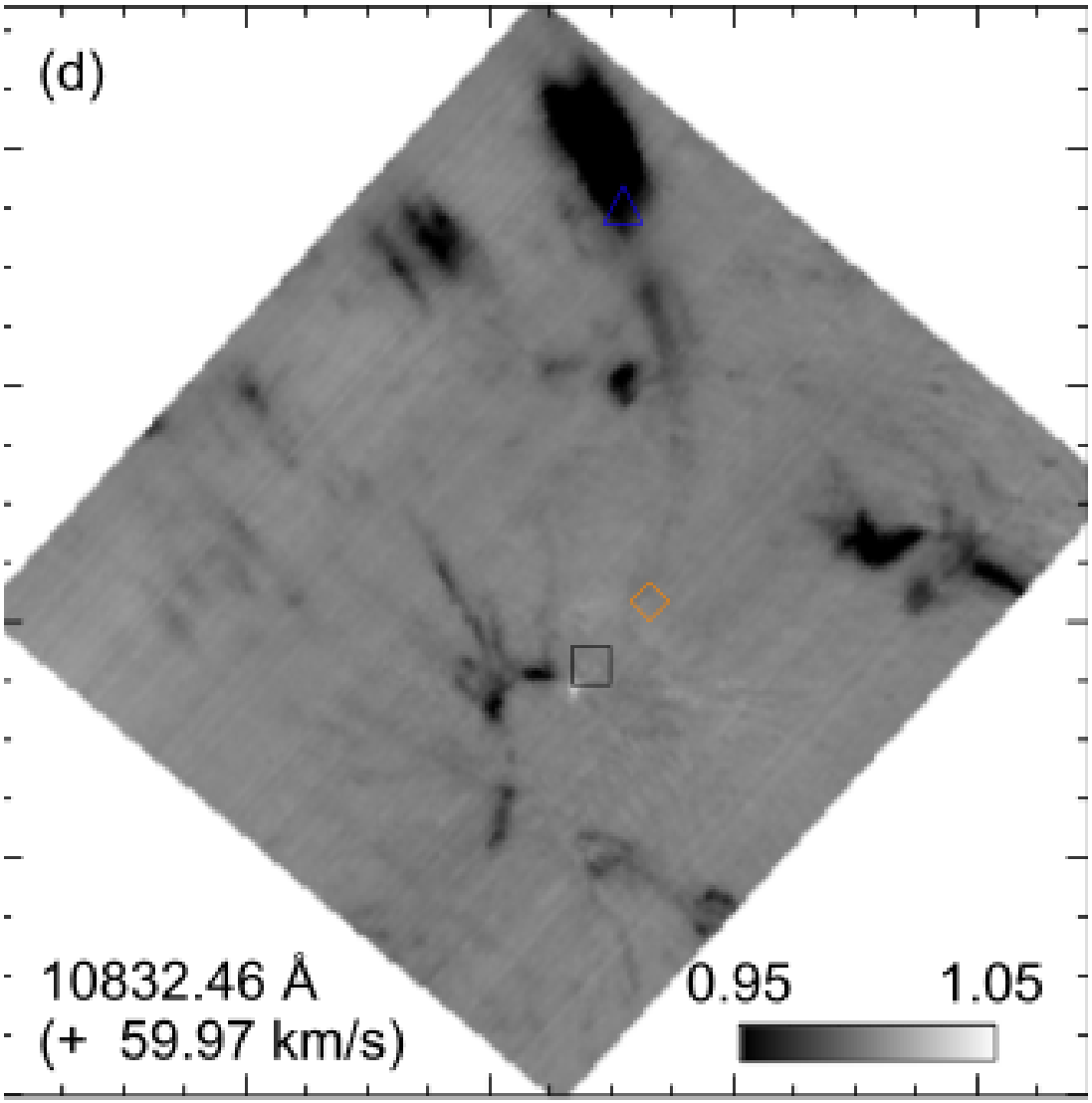

He velocity along loop

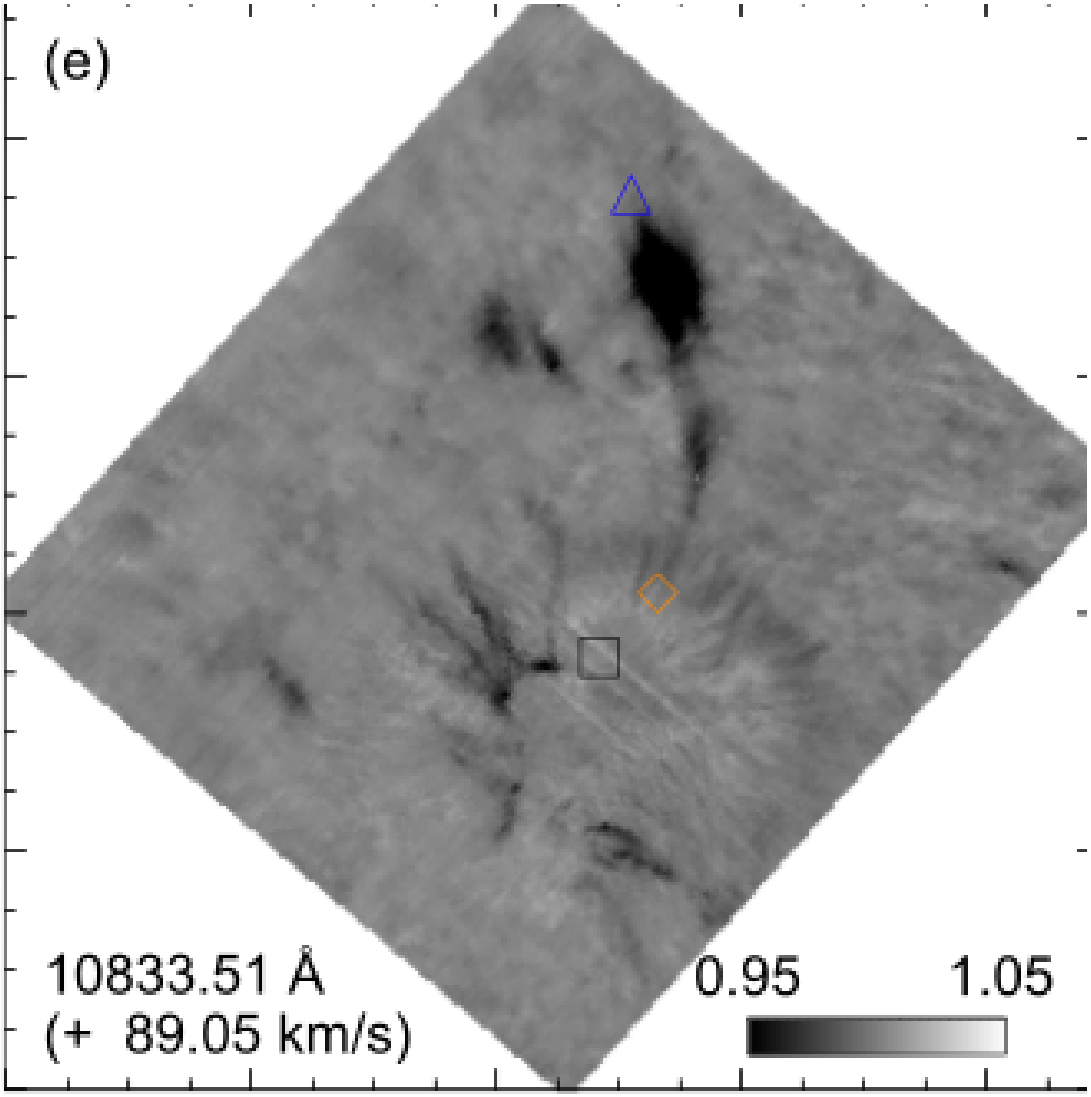

He velocity along loop

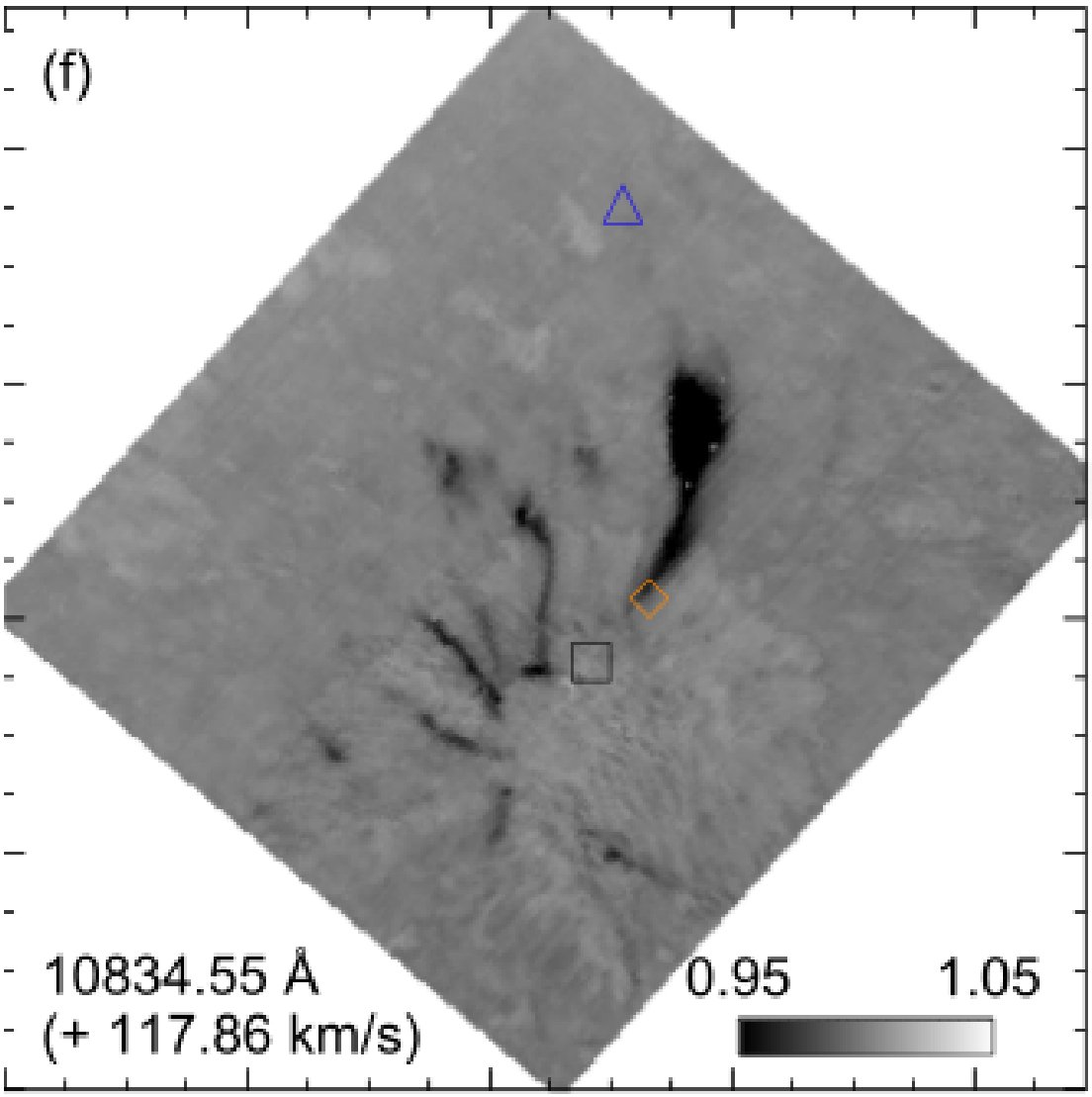

He velocity along loop

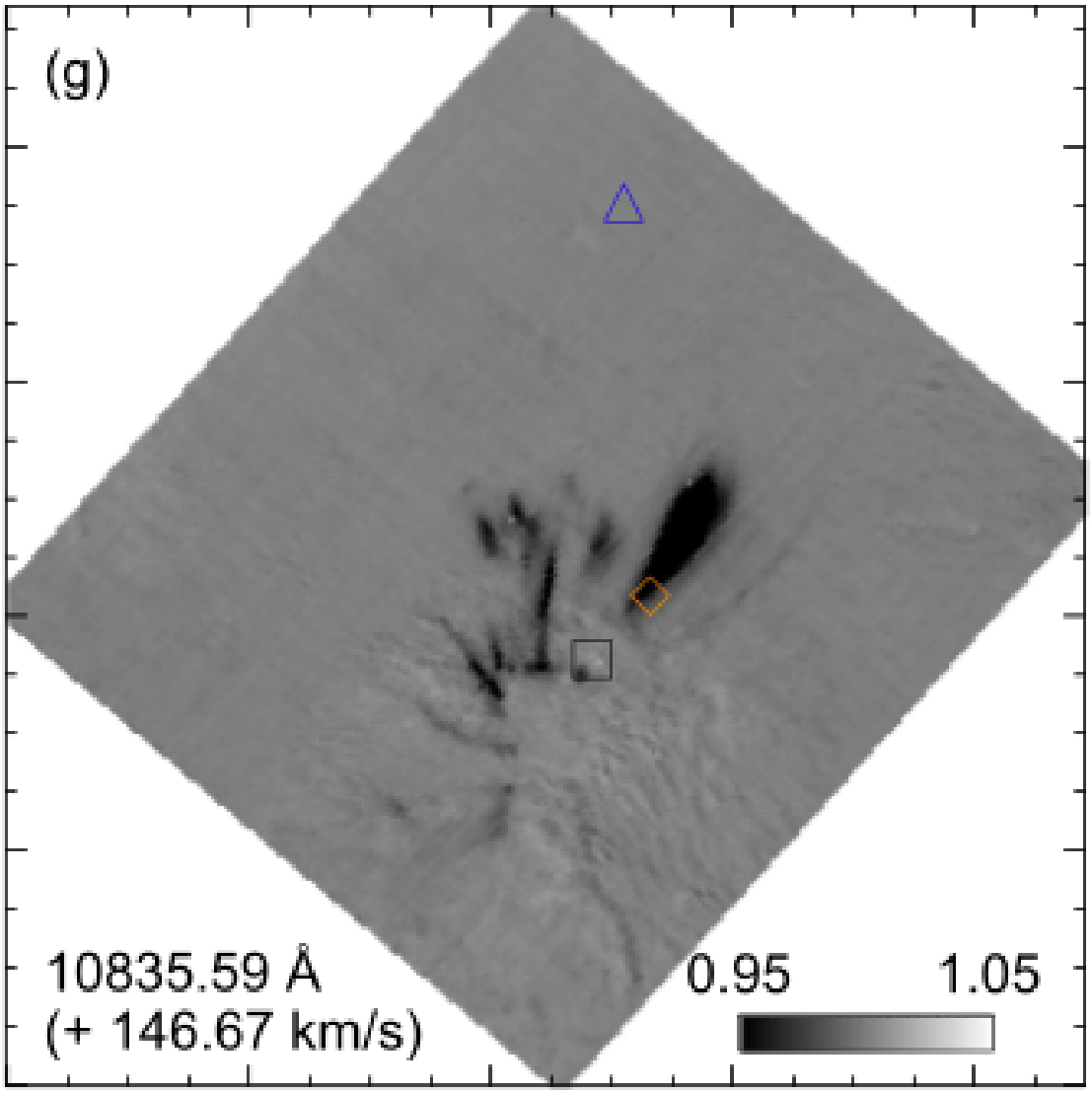

He velocity along loop

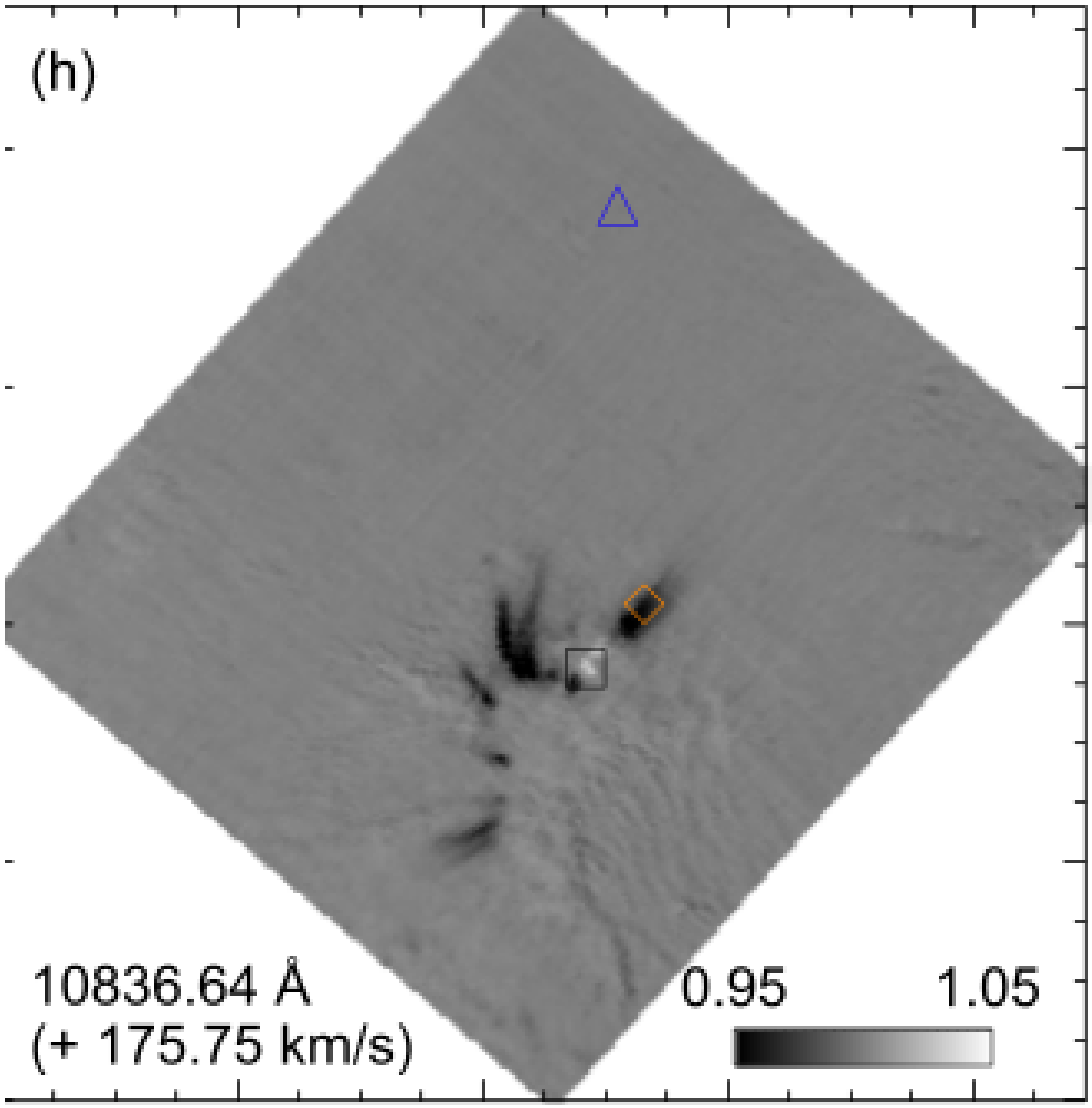

He velocity along loop

normalized to the local continuum intensity

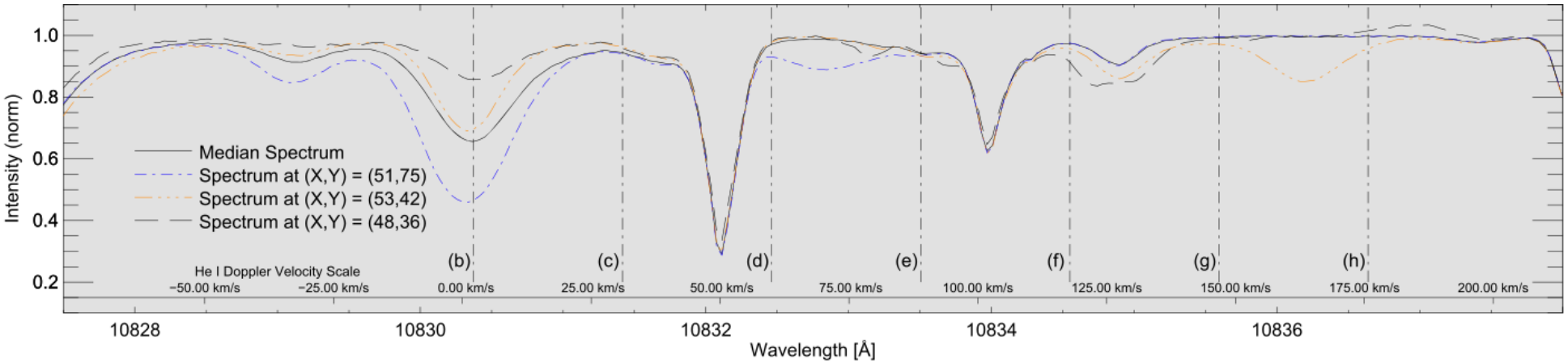

Figure 1: spectral line profiles extracted from the locations indicated in panels (a)(h), illustrating the presence of additional He I velocity components redward of the telluric feature at 10832.1 Å, and relative to the median spectrum calculated using the entire data cube. An He I Doppler velocity scale bar is added for reference

Stereoscopic observations

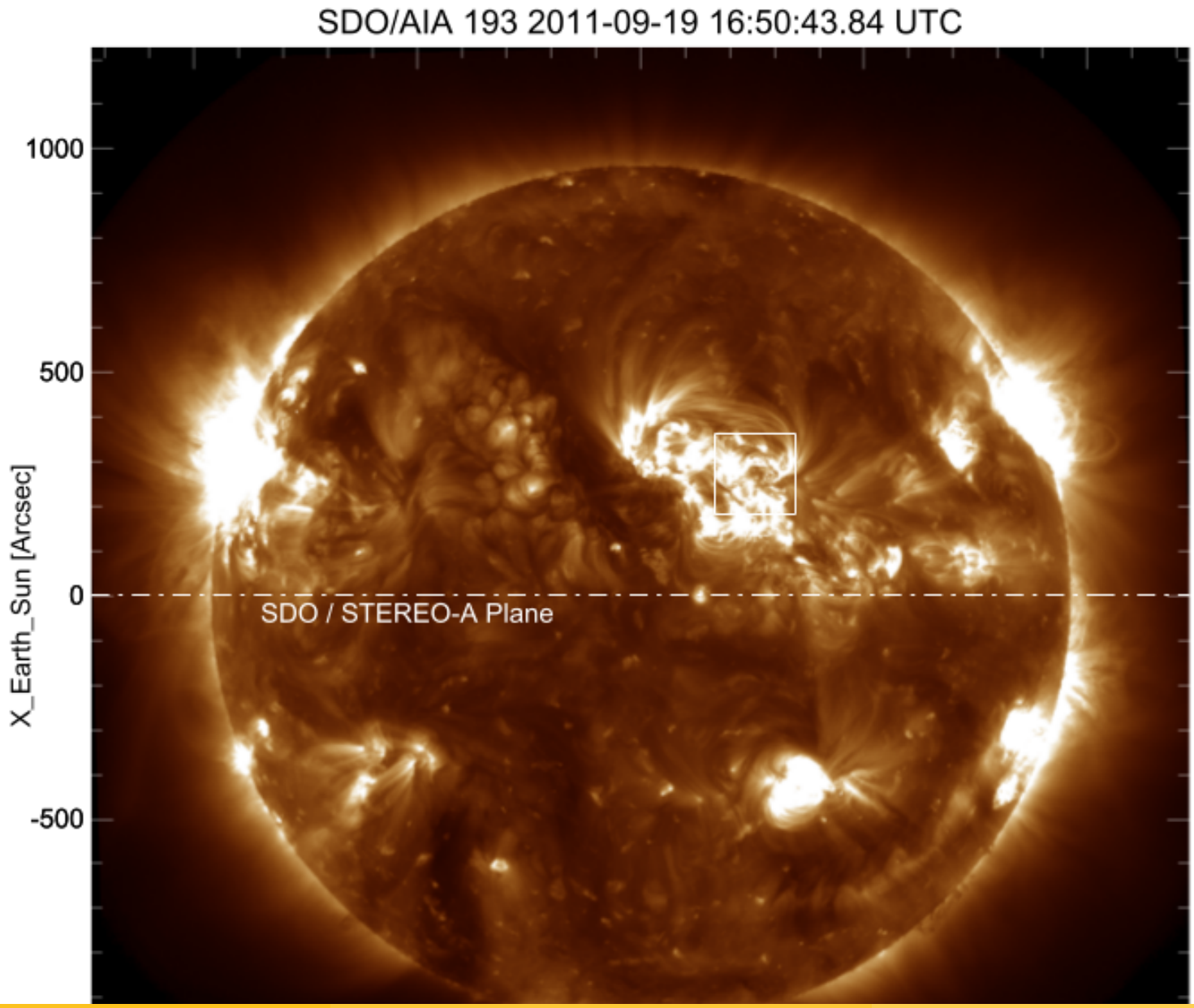

Stereoscopic observations